Journal of Orthopaedic Translation 49 (2024) 23–36

Contents lists available at ScienceDirect

Journal of Orthopaedic Translation

journal homepage: www.journals.elsevier.com/journal-of-orthopaedic-translation

Original Article

Human umbilical cord mesenchymal stem cell-derived exosomes ameliorate muscle atrophy via the miR-132-3p/FoxO3 axis

Huihui Ma [a,1], Yujie Jing [a,1], Jiangping Zeng [a], Jiaying Ge [a], Siqi Sun [a], Ran Cui [a], Chunhua Qian [a], Shen Qu [a], Hui Sheng [a,b,*]

[a] Department of Endocrinology and Metabolism, Shanghai Tenth People's Hospital, School of Medicine, Tongji University, Shanghai, 200072, China
[b] Department of Endocrinology and Metabolism, Anqing Traditional Chinese Medicine Hospital, Anqing Medical College, Anqing, 246052, China

ARTICLE INFO

Keywords:
Exosomes
FoxO3
Human umbilical cord mesenchymal stem cells
Muscle atrophy
MiR-132-3p
Sarcopenia

ABSTRACT

Background: Muscle atrophy or sarcopenia is the loss of muscle mass and strength and leads to an increased risk of disability and death including osteoporotic fractures. Currently, there are no available clinical biologic agents for the treatment of sarcopenia. Since exosomes have become increasingly attractive as a novel therapeutic approach due to their ability to facilitate cell-cell transfer of proteins and RNAs, promoting cell repair and function recovery, we hypothesized that human umbilical cord mesenchymal stem cell-derived exosomes (hucMSC-Exos) might benefit muscle atrophy in age-related and dexamethasone-induced sarcopenia animal models.

Methods: HucMSC-Exos were harvested by ultrafast centrifugation and identified by transmission electron microscopy, particle size analysis, and Western blot analysis. The effects of hucMSC-Exos on muscle atrophy were evaluated using age-related and dexamethasone-induced muscle atrophy mice models. Body weight, grip strength, muscle weight, and muscle histology of these mice were assessed. The expression levels of muscle RING finger 1 (MuRF1) and muscle atrophy F-box (atrogin-1) were measured by Western blot. Dexamethasone-induced C2C12 myotube atrophy was used to establish the cell model of muscle atrophy. Myotube diameter was evaluated by immunofluorescence staining. Bioinformatic analysis, RNA sequencing analysis, and Western blot analysis were performed to explore the underlying mechanisms.

Results: In vivo experiments, hucMSC-Exos demonstrated a remarkable capacity to improve grip strength, increase muscle mass, and muscle fiber cross-sectional area, while concurrently reducing the expression of MuRF1 and atrogin-1 in age-related and dexamethasone-induced muscle atrophy mice. In vitro experiments, hucMSC-Exos can promote the proliferation of C2C12 cells, and rescue the dexamethasone-induced decline in the viability of C2C12 myotubes. In addition, hucMSC-Exos can increase the diameter of C2C12 myotubes, and reduce dexamethasone-induced upregulation of MuRF1 and atrogin-1. Combined with bioinformatics analysis and RNA sequencing analysis, we further showed that miR-132-3p was one of the essential miRNAs in hucMSC-Exos and played an important role by targeting FoxO3.

Conclusion: Our findings suggested that hucMSC-Exos can improve age-related and dexamethasone-induced muscle atrophy in mice models. This study first demonstrated that hucMSC-Exos may ameliorate muscle atrophy via the miR-132-3p/FoxO3 axis. These data may provide novel and valuable insights into the clinical transformation of hucMSC-Exos for the treatment of sarcopenia.

The translational potential of this article: HucMSC-Exos are easily available for clinical application, this study further consolidates the evidence for the clinical transformation potential of hucMSC-Exos for sarcopenia and provides its new target pathway.

1. Introduction

Muscle atrophy or sarcopenia occurs under various conditions, including aging [1], denervation [2], cancer [3], and drug treatment [4], which can lead to diminished physical performance, reduced quality of life, and increased risk of fractures [5]. According to the Asian

* Corresponding author.
E-mail address: shenghui@tongji.edu.cn (H. Sheng).
[1] Contributed equally

https://doi.org/10.1016/j.jot.2024.08.005
Received 10 December 2023; Received in revised form 5 August 2024; Accepted 5 August 2024

Working Group for Sarcopenia (AWGS) 2014 criteria, the prevalence of sarcopenia in Asian countries ranged from 5.5 % to 25.7 % [6]. Studies have confirmed that osteoporosis and sarcopenia (osteosarcopenia) often occur together in older people, and osteosarcopenia is associated with severe physical disability [7]. In a cohort study of Finnish post-menopausal women, women with sarcopenia had a 12.9 times higher risk of developing osteoporosis compared to those without sarcopenia [8]. In addition, a study in Taiwan found a higher risk of osteoporotic fractures in patients with sarcopenia after adjusting for possible confounding factors [9]. Therefore, sarcopenia increases the risk of fractures in patients with osteoporosis, which poses a serious health and economic burden. However, at present, there are no available clinical biologic agents for the treatment of sarcopenia.

Mesenchymal stem cells (MSCs) have been used to treat various diseases, compared with other sources, human umbilical cord mesenchymal stem cells (hucMSCs) are the preferred candidates for cell therapy due to the non-invasive isolation method, lower immunogenicity, and higher proliferation ability. However, hucMSCs have faced limitations related to transportation difficulties and safety concerns in clinical treatment [10,11]. Recent studies have shown that extracellular vesicles from MSCs have regenerative functions in many tissues including the liver and lung [12,13]. Exosomes are important components of extracellular vesicles, ranging in diameter from 30 to 150 nm and containing DNA, RNA, lipids, and proteins [14,15]. Exosomes secreted by stem cells have been shown to function similarly as stem cells, but avoid potential risks during cell transplantation [16]. Studies have shown that human umbilical cord mesenchymal stem cells-derived exosomes (hucMSC-Exos) promote structural and functional repair of cells, and hucMSC-Exos treatment significantly improve neurological function and facilitate remyelination [17]. In a mouse model of natural ovarian aging, ovarian function was improved after treatment with hucMSC-Exos, such as recovery of follicle number and hormone levels [18]. Therefore, we hypothesized that hucMSC-Exos could potentially ameliorate age-related and dexamethasone-induced muscle atrophy.

A growing number of studies have already confirmed that exosomal microRNAs (miRNAs) mediate intracellular communication. MiRNAs are short-chain RNA molecules that play a vital role in regulating the transcriptome, which can induce gene silencing by complementarily targeting the 3′ untranslated region (UTR) of target mRNAs [19]. Therefore, we hypothesized that hucMSC-Exos may ameliorate muscle atrophy by carrying miRNAs. We validated the efficacy of hucMSC-Exos therapy through animal models of age-related and dexamethasone-induced muscle atrophy, respectively. Further studies found that hucMSC-Exos may ameliorate muscle atrophy, at least in part, via the miR-132-3p/FoxO3 axis. These results provide fresh perspectives for understanding the role of hucMSC-Exos in the treatment of sarcopenia.

2. Materials and methods

2.1. Animals and treatments

All animal studies were approved by the Animal Care and Use Committee of Shanghai Tenth People's Hospital. Male C57BL/6 mice aged 6 weeks were purchased from Shanghai Bikai Laboratory Animal Co. Ltd. All animals were housed in a specific pathogen-free (SPF) environment under 12 h light-dark cycles, and given food and water ad libitum. For the dexamethasone-induced muscle atrophy animal model, after two weeks of adaptive feeding, thirty 8-week-old mice were randomly divided into three groups (n = 10): (a) the control group (CON); (b) the dexamethasone treatment group (DEX); (c) the dexamethasone + exosomes treatment group (DEX + Exos). The mice were intraperitoneally injected with dexamethasone (20 mg/kg) once a day for 14 days. For exosomes injection, 40 μg exosomes were injected via the tail vein every 3 days starting one day before dexamethasone administration, and this treatment was performed for 15 days. For the age-related muscle atrophy animal model, ten male C57BL/6 mice were randomly divided into two groups (n = 5) when they grew up to 20 months old: (a) the control group (CON); and (b) the exosomes treatment group (Exos). For exosomes injection, 20 μg exosomes were injected via the tail vein every 3 days, and this treatment was performed for 8 weeks. At the end of the experiment, three types of muscle tissues, including gastrocnemius (GA), tibialis anterior (TA), and quadriceps femoris (QD), were isolated and weighed. GA muscle was immediately frozen in liquid nitrogen and maintained at −80 °C. The atrophy rate was calculated by the ratio of muscle weight (mg) to body weight (g).

2.2. Grip strength test

At the end of the experiment, a grip strength test was performed to evaluate the muscle strength using a grip strength meter (SA417, SANS Biological Technology Co. Ltd.). The mice were placed on the force meter allowing four paws to grip the grid and then slowly dragged backward until it could no longer hold on to it. Three tests were performed on each mouse, and the average value was analyzed statistically.

2.3. Hematoxylin and eosin (H&E) and Masson staining

GA tissue was fixed with 4 % paraformaldehyde for 24 h and embedded in paraffin. Transverse GA sections were stained with HE. The cross-sectional area (μm^2) of the muscle fibers was quantified using ImageJ software. Masson staining was performed to determine fibrosis in the GA muscle and the area of fibrosis was quantitatively analyzed using ImageJ software.

2.4. HucMSCs culture and identification

HucMSCs were purchased from Yuanchuang Biotechnology (Shanghai, China) and were cultured in icell primary mesenchymal stem cell serum-free basic culture medium (PriMed-iCell-012-SF, Saibaikang) supplemented with 5 % nutritional additives. HucMSCs were maintained in the condition of 5 % CO_2 at 37 °C. The morphology of hucMSCs was observed by optical microscopy. Flow cytometry was used to identify the surface markers in hucMSCs. CD29 and CD90 were used as positive markers, and CD45 and CD31 were used as negative markers. All antibodies were acquired from BioLegend: CD29 R-phycoerythrin (PE), 303003; CD90 brilliant violet 421, 328121; CD45 allophycocyanin (APC), 304011; CD31 fluorescein isothiocyanate (FITC), 303103.

2.5. Isolation, characterization, and transfection of hucMSC-Exos

HucMSCs in passages 3–8 were used for the study. The culture supernatant was collected and exosomes were isolated by differential ultracentrifugation [20]. Briefly, the supernatant was centrifuged at 300×*g* for 10 min, 2000×*g* for 10 min, 10,000×*g* for 30 min, and 100,000×*g* for 70 min at 4 °C. Pelleted vesicles were resuspended in cold phosphate buffered saline (PBS) and ultracentrifuged at 100,000×*g* for 70 min at 4 °C again. The exosome pellet was resuspended in 200 μL PBS and stored at −80 °C for further experiments. The total protein concentration of exosomes was measured by a bicinchoninic acid (BCA) protein assay kit (ZJ101, Epizyme). The amount and size of exosomes were measured by nanoparticle tracking analysis (NTA). The morphology of exosomes was observed by transmission electron microscopy (TEM). Transfection of exosomes was performed using Exo-Fect™ siRNA/miRNA Transfection Kit (EXFT200A-1, SBI) according to the manufacturer's instructions.

2.6. Intracellular uptake of hucMSC-Exos

HucMSC-Exos were labeled with CellMask (C10046, TermoFisher Scientific). Briefly, the exosomes were incubated at 37 °C for 15 min in the presence of CellMask, and the unbound dyes were removed by

ultracentrifugation at 100,000×*g* for 70 min. After washing with PBS, the labeled exosomes were resuspended in PBS. In the internalization experiment, C2C12 myoblasts and C2C12 myotubes were treated with the labeled exosomes, stained with 4′, 6-diamidino-2-phenylindole (DAPI) and phalloidin. A confocal microscope was used for observing the internalization of the hucMSC-Exos.

2.7. C2C12 cell culture and differentiation

Mouse C2C12 myoblasts were a gift from Chaobao Zhang of Shanghai Key Laboratory of Clinical Geriatric Medicine and were cultured in Dulbecco's modified Eagle's medium (DMEM, C11995500CP, Gibco) supplemented with 10 % fetal bovine serum (FBS, 16000–044, Gibco), 100 U/mL penicillin, and 100 μg/mL streptomycin (15140–122, Gibco). For the induction of differentiation into myotubes, the cells were incubated with DMEM containing 2 % horse serum (HS, SH30074.03, Hyclone) for 6 days.

2.8. Treatment with exosomes and dexamethasone

The differentiated myotubes were divided into four groups: the control group (CON), in which cells were cultured in serum-free medium (SFM; DMEM containing 100 U/mL penicillin and 100 μg/mL streptomycin); the exosomes treatment group (Exos), in which cells were treated with 40 μg/mL exosomes; the dexamethasone treatment group (DEX), in which cells were treated with 10 μM dexamethasone; and the dexamethasone + exosomes treatment group (DEX + Exos), in which cells were treated with 10 μM dexamethasone and 40 μg/mL exosomes. All groups were incubated in a serum-free medium at 37 °C with 5 % CO_2 for 24 h, and then cells were harvested for the experiment.

2.9. Cell viability assay

Cell viability was determined using the Cell Counting Kit-8 (CCK-8, C0042, Beyotime) according to the manufacturer's instructions. Briefly, C2C12 cells were seeded in 96-well plates. Then, 10 μL of CCK-8 was added to each well and incubated at 37 °C for 1 h, and the absorbance was measured at 450 nm with a plate reader.

2.10. Immunofluorescence and myotube diameter measurement

C2C12 myotubes were fixed for 15 min in 4 % paraformaldehyde, permeabilized with 0.5 % Triton X-100 for 20 min, and blocked in 1 % bovine serum albumin (BSA) for 1 h before staining with MyHC primary antibody (1:100, sc-376157, Santa Cruz) overnight at 4 °C. C2C12 myotubes were incubated with appropriate secondary antibody for 1 h. Nuclear counterstaining was performed with DAPI. The myotubes were photographed under a Leica fluorescence microscope. The diameters were measured in at least 50 myotubes from at least 10 random fields using ImageJ software [21].

2.11. Western blot

Total proteins were extracted using RIPA lysis buffer (P0013B, Beyotime) supplemented with protease inhibitors (P8340, Sigma). Protein concentration was quantified using a BCA protein assay kit (ZJ101, Epizyme). 20 μg protein was loaded onto sodium dodecyl sulfate-polyacrylamide gel and separated by electrophoresis. The proteins were transferred onto polyvinylidene fluoride (PVDF) membranes and subsequently blocked using 5 % nonfat milk for 2 h at room temperature, and then incubated overnight at 4 °C with appropriate primary antibodies and incubated with the corresponding secondary antibodies for 1 h at room temperature. Then, the membranes were visualized by enhanced chemiluminescence (ECL) detection reagents (P0018FS, Beyotime). The grayscale densities of the protein bands were quantified using ImageJ software.

The primary antibodies were as follows: anti-CD63 (1:1000, ab271286, Abcam), anti-Tsg101 (1:1000, ab125011, Abcam), anti-Alix (1:1000, ab275377, Abcam), anti-GAPDH (1:10000, 60004-1-Ig, Proteintech), anti-FoxO3 (1:2000, 10849-1-AP, Proteintech), anti-MuRF1 (1:500, sc-398608, Santa Cruz), anti-Atrogin-1 (1:1000, ab168372, Abcam), The secondary antibodies were anti-mouse IgG (1:2000, SA00001-1, Proteintech) and anti-rabbit IgG (1:2000, SA00001-2, Proteintech).

2.12. RNA extraction and quantitative real-time PCR

Extraction of total RNA was performed using TRIzol (15596026, Invitrogen). Complementary DNA (cDNA) was synthesized using PrimeScript™ RT reagent kit (RR037A, Takara). Real-time quantitative PCR was conducted with the real-time PCR kit (RR820A, Takara). For the analysis of mRNAs, GAPDH was amplified as an internal control. For the quantitative analysis of miRNAs, Bulge-Loop miRNA RT primer was used. The relative expression levels of miRNAs were normalized against that of U6. The primer of U6 and miR-132-3p were purchased from RiboBio (Guangzhou, China). The relative expression levels were calculated using the $2^{-\Delta\Delta CT}$ method.

The primer sequences were as follows: GAPDH-F: AACTTTGGCATTGTGGAAGG, GAPDH-R: ACACATTGGGGGTAGGAACA; MuRF1-F: GTGTGAGGTGCCTACTTGCTC, MuRF1-R: GCTCAGTCTTCTGTCCTTGGA; Atrogin-1-F: CAGCTTCGTGAGCGACCTC, Atrogin-1-R: GGCAGTCGAGAAGTCCAGTC; FoxO3-F: CTGGGGGAACCTGTCCTATG, FoxO3-R: TCATTCTGAACGCGCATGAAG.

2.13. RNA sequencing

Total RNA was extracted using the TRIzol reagent (Invitrogen, USA) according to the manufacturer's protocol. The RNA libraries were sequenced by OE Biotech, Inc., Shanghai, China. DESeq2 was applied to perform the differential expression analysis. The standards for differential expression genes were set as p value < 0.05 and $|\text{Foldchange}| > 1.5$. Hierarchical cluster analysis of differential expression genes was performed using R (v 3.2.0) to demonstrate the expression pattern of genes in different groups and samples. Based on the hypergeometric distribution, Gene Ontology (GO) and Kyoto Encyclopedia of Genes and Genomes (KEGG) pathway enrichment analysis of differential expression genes were performed to screen the significantly enriched term using R (v 3.2.0), respectively.

2.14. Statistical analysis

All data were expressed as mean ± standard deviation (SD) and analyzed by GraphPad Prism 6 software. The Kolmogorov–Smirnov test was used to evaluate the normality of the distribution. Statistical analysis was performed by unpaired student's t-test or Mann–Whitney U test for two groups, and one-way analysis of variance (ANOVA) or the Kruskal–Wallis test for multiple groups. Two-tailed p values < 0.05 were considered statistically significant.

3. Results

3.1. Isolation and identification of the hucMSC-Exos

HucMSCs were cultured in good condition, and the cells passaged to the 4th generation were spindle-shaped (Fig. 1A). Flow cytometry detected cell surface antigen markers, and the results showed that CD29 and CD90 were highly expressed, while CD31 and CD45 were lowly expressed (Fig. 1B). Exosomes were extracted from the hucMSCs culture supernatant. Western blot analysis showed that exosome markers Tsg101, Alix, and CD63 were expressed in hucMSC-Exos (Fig. 1C). TEM was used to confirm the morphology of hucMSC-Exos (Fig. 1D). NTA showed the particle diameter distribution range of hucMSC-Exos

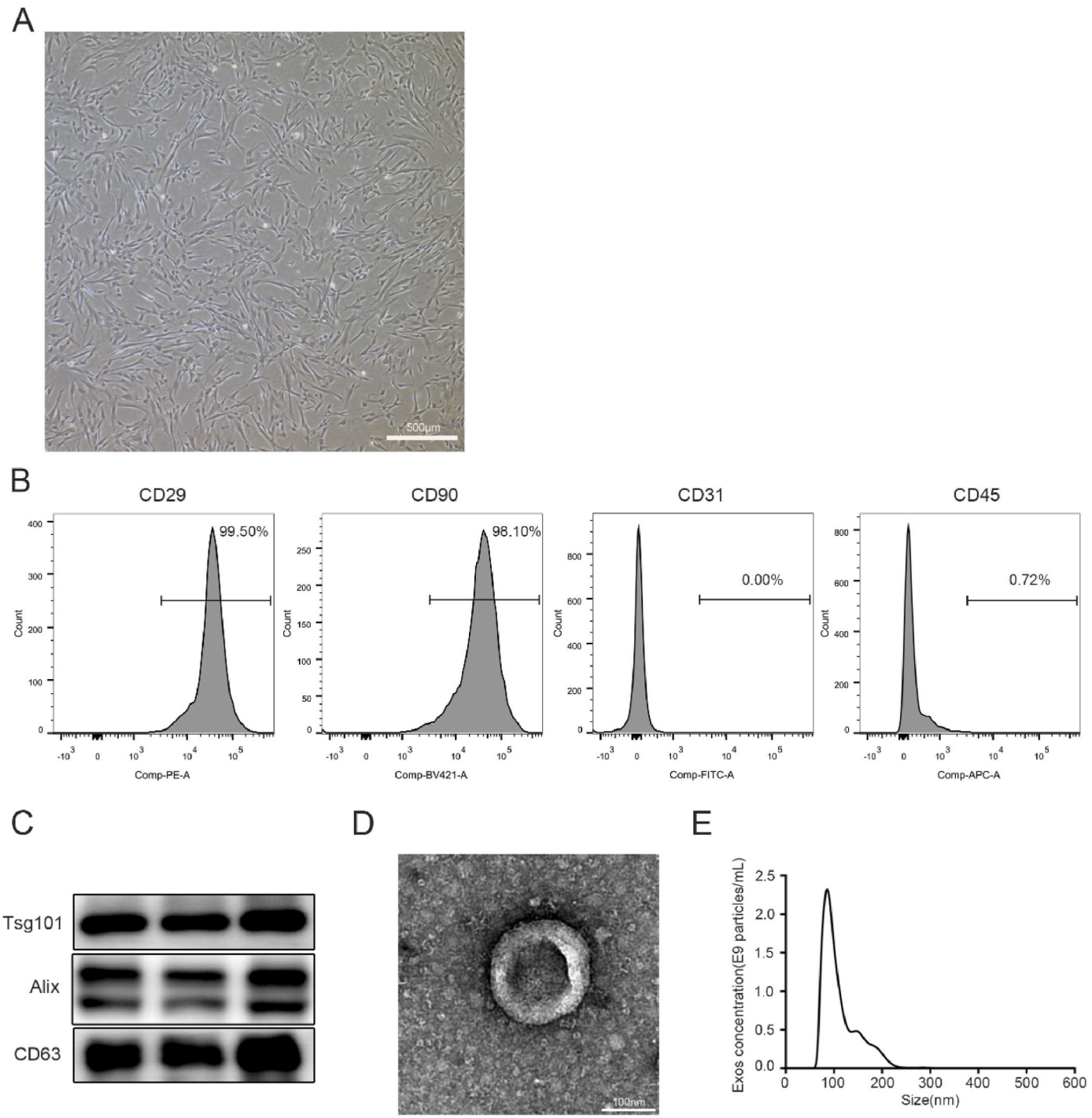

Figure 1. Isolation and identification of the hucMSC-Exos (A) The morphology of hucMSCs under an inverted microscope at the 4th generation. Scale bar = 500 μm (B) Flow cytometry analysis showed the expression of surface antigen markers for hucMSCs (CD29, CD90, CD31, and CD45) (C) Protein markers of hucMSC-Exos were confirmed by Western blot (Tsg101, Alix, and CD63) (D) The representative images of hucMSC-Exos under a TEM. Scale bar = 100 nm (E) The particle diameter distribution range of hucMSC-Exos detected by NTA.

(Fig. 1E). These results indicate that hucMSC-Exos were isolated.

3.2. HucMSC-Exos alleviate loss of muscle strength and muscle weight in age-related muscle atrophy in mice

To investigate the effect of hucMSC-Exos on age-related muscle atrophy, we injected 20-month-old mice with hucMSC-Exos by the tail vein every three days for eight weeks. We separated and weighed three muscle tissues, namely TA, GA, and QD muscle. While hucMSC-Exos treatment did not significantly affect overall body weight, it led to an increase in the weight of TA, GA, and QD muscles (Fig. 2B–E). HucMSC-Exos treatment improved grip strength (Fig. 2A) and increased the cross-sectional area of muscle fibers in age-related muscle atrophy mice (Fig. 2F–H). In addition, hucMSC-Exos treatment reduced the development of muscle fibrosis (Fig. 2I and J). To determine whether hucMSC-Exos therapy can change the expression of muscle atrophy-associated factors, we used Western blot and found that hucMSC-Exos can reduce the upregulation of MuRF1 and atrogin-1 protein levels in age-related

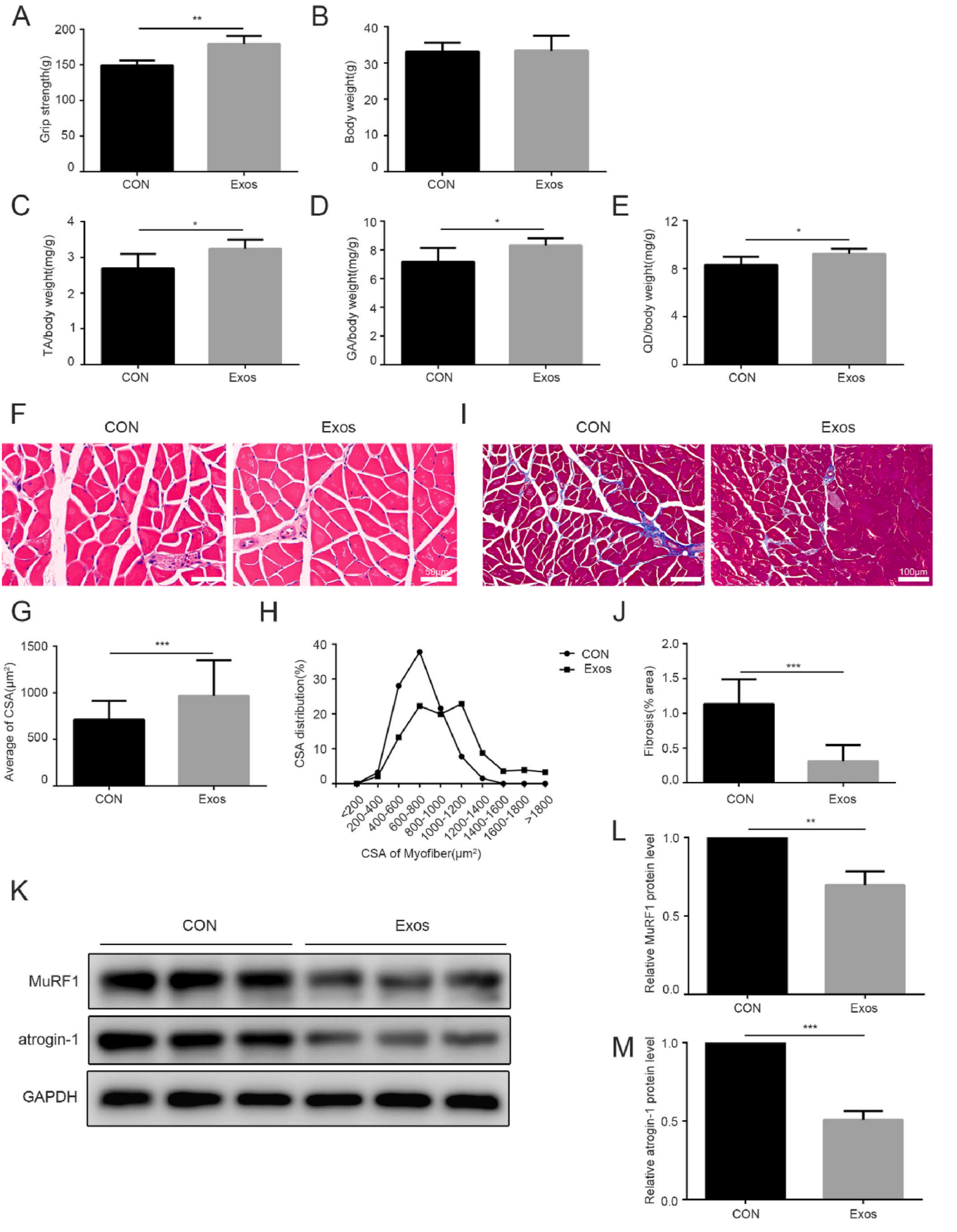

(caption on next page)

Figure 2. HucMSC-Exos alleviate age-related muscle atrophy (A) Grip strength test (n = 5 in each group) (B) Body weight of mice (n = 5 in each group) (C–E) Muscle weights of the tibialis anterior (TA) (C), gastrocnemius (GA) (D), and quadriceps femoris (QD) (E) were measured and normalized to body weight (n = 5 in each group) (F) A representative picture of H&E staining. Scale bar = 50 μm (n = 3 in each group) (G) The cross-sectional area (CSA) of muscle fibers was measured by ImageJ software (H) Muscle fiber size distribution (I) A representative picture of Masson staining. Scale bar = 100 μm (n = 3 in each group) (J) Quantitative analysis of the area of fibrosis using ImageJ software (K–M) The protein expression levels of MuRF1 and atrogin-1 were detected by Western blot (n = 3 in each group). GAPDH was used as an internal control. The relative protein expression level was quantified by ImageJ software. Data are presented as the mean ± SD, $^{*}p < 0.05$, $^{**}p < 0.01$, $^{***}p < 0.001$.

muscle atrophy mice (Fig. 2K–M). These results indicate that hucMSC-Exos therapy can effectively improve age-related muscle atrophy.

3.3. HucMSC-Exos alleviate loss of muscle strength and muscle weight in dexamethasone-induced muscle atrophy in mice

To explore the effect of hucMSC-Exos on dexamethasone-induced muscle atrophy, we injected 8-week-old mice with hucMSC-Exos through the tail vein the day before intraperitoneal injection of dexamethasone, once every three days for 15 days. We separated and weighed three muscle tissues, namely TA, GA, and QD muscle. While hucMSC-Exos treatment did not significantly affect overall body weight, it led to an increase in the weight of TA, GA, and QD muscles (Fig. 3B–E). HucMSC-Exos treatment improved grip strength (Fig. 3A) and increased muscle fiber cross-sectional area in dexamethasone-induced muscle atrophy mice (Fig. 3F–H). In addition, hucMSC-Exos treatment reduced the development of muscle fibrosis (Fig. 3I and J). To determine whether hucMSC-Exos treatment can change the expression of muscle atrophy-associated factors, Western blotting detection was used to find that hucMSC-Exos can reduce the dexamethasone-induced upregulation of MuRF1 and atrogin-1 protein levels (Fig. 3K–M). These results indicate that hucMSC-Exos therapy can effectively improve dexamethasone-induced muscle atrophy.

3.4. HucMSC-Exos promote the proliferation of C2C12 cells and rescue the dexamethasone-induced decline in the viability of C2C12 myotubes

We analyzed whether hucMSC-Exos can be internalized by C2C12 cells and myotubes, hucMSC-Exos were labeled with the fluorescence dye CellMask and co-cultured with C2C12 cells and myotubes. Red fluorescence was observed in the C2C12 cells and myotubes, which proved that hucMSC-Exos were internalized by C2C12 cells and myotubes (Fig. 4A). To study the effect of hucMSC-Exos on cell function, we used a culture medium containing FBS as the positive control and treated C2C12 cells with culture media containing different concentrations of hucMSC-Exos without FBS. According to the results of the CCK-8 assay, the proliferation index of C2C12 cells increased in a concentration-dependent manner, and when the concentration of hucMSC-Exos reached 40 μg/mL or above, the cell proliferation index significantly increased, indicating that hucMSC-Exos promoted the proliferation of C2C12 cells (Fig. 4B).

To study the effect of hucMSC-Exos on myotube atrophy, firstly we treated C2C12 myotubes with dexamethasone at different concentrations. We found that dexamethasone at 10 μM concentration led to a significant increase in MuRF1 and atrogin-1 regardless of RNA level or protein level (Fig. 4C–G). In addition, the cell viability also decreased significantly (Fig. 4H), so we chose 10 μM dexamethasone for subsequent cell experiments. In addition, we found that hucMSC-Exos rescued the dexamethasone-induced decline in the viability of C2C12 myotubes when hucMSC-Exos concentrations reached 40 μg/mL and above (Fig. 4I). Thus, hucMSC-Exos can promote the proliferation of C2C12 cells and rescue the dexamethasone-induced decline in the viability of C2C12 myotubes.

3.5. HucMSC-Exos rescue dexamethasone-induced myotube atrophy

To study the effect of hucMSC-Exos on myotube atrophy, we observed myotube diameter by immunofluorescence staining. The results showed that the diameter of dexamethasone-treated C2C12 myotubes decreased, while hucMSC-Exos treatment increased the myotubes diameter (Fig. 5A and B). We then further evaluated whether hucMSC-Exos treatment could alter the expression of muscle atrophy-related factors. The results showed that dexamethasone treatment significantly increased the expression of MuRF1 and atrogin-1 at both RNA and protein levels, whereas hucMSC-Exos treatment significantly reduced dexamethasone-induced upregulation of MuRF1 and atrogin-1 mRNA and protein levels (Fig. 5C–G). These results confirmed that hucMSC-Exos rescued dexamethasone-induced myotube atrophy.

3.6. MiR-132-3p derived from hucMSC-Exos inhibits dexamethasone-induced myotube atrophy by targeting FoxO3

As one of the most important contents in exosomes, miRNAs exert their biological role by inhibiting the expression and function of target genes and play an important role in regulating metabolic diseases, such as diabetes mellitus [22] and polycystic ovary syndrome [23]. Therefore, to investigate the possible mechanism by which hucMSC-Exos affect muscle atrophy, we analyzed the expression of the top 200 miRNAs in the datasets GSE153752, GSE159814, GSE211008, and GSE69909. A total of 90 miRNAs were found to be highly expressed in all four datasets (Fig. 6A). Next, to explore the molecular mechanism of dexamethasone-induced muscle atrophy, transcriptome sequencing was performed on the dexamethasone-treated group and the blank control group in the myotubes formed by C2C12 differentiation. Principal component analysis showed a significant difference between the dexamethasone group and the control group (Fig. 6B). Compared with the control group, 932 genes were up-regulated and 1151 genes were down-regulated in the dexamethasone group (Fig. 6C). We did a GO enrichment analysis and a KEGG pathway analysis of these differential genes, GO analysis showed that these differential genes were mainly enriched in an extracellular matrix organization, skeletal system development, etc (Fig. 6D). According to the KEGG pathway analysis, the up-regulated genes list included the FoxO signaling pathway, and the list of down-regulated genes included the PI3K-AKT signaling pathway in the top 20 functionally enriched KEGG pathways (Fig. 6E and F). FoxO signaling pathway plays an important role in muscle atrophy, and the PI3K/AKT pathway regulates FoxO transcription factors, up-regulates the expression of MuRF1 and atrogin-1, and increases the breakdown of muscle protein. Therefore, we next explored the role of the FoxO family in using hucMSC-Exos to regulate skeletal muscle function.

FoxO3, a member of the FoxO family, is overactivated in some disease processes. FoxO3 is required for the transcription of atrogin-1 and MuRF1, which can induce muscle atrophy by up-regulating the expression of atrogin-1 and MuRF1 [24,25]. Therefore, we first treated C2C12 myotubes with dexamethasone at different concentrations. We found that dexamethasone at 10 μM concentration led to a significant increase in FoxO3 regardless of RNA level or protein level (Fig. 7A–C). Next, we detected the expression of FoxO3 after hucMSC-Exos treatment and found that the expression of FoxO3 at both mRNA and protein levels was up-regulated after dexamethasone treatment of myotubes, while FoxO3 expression was down-regulated after hucMSC-Exos treatment, indicating that hucMSC-Exos might rescue dexamethasone induced-myotube atrophy by regulating FoxO3 (Fig. 7D–F). So, we used the TargetScan database to predict the miRNAs targeting FoxO3. We identified five miRNAs with conserved binding sites to FoxO3 and

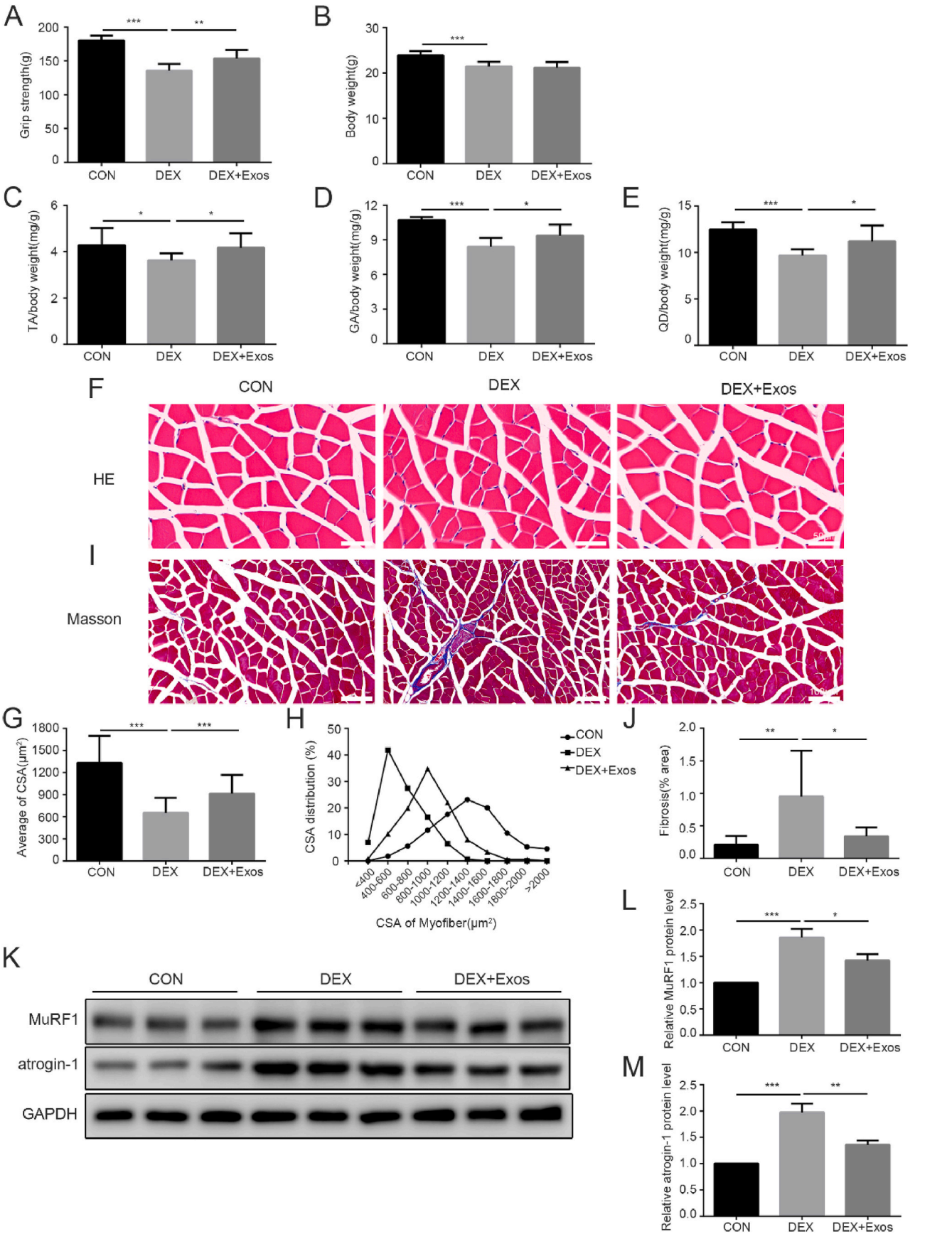

(caption on next page)

Figure 3. HucMSC-Exos alleviate muscle atrophy induced by dexamethasone (A) Grip strength test (n = 8–10 in each group) (B) Body weight of mice (n = 8–10 in each group) (C–E) Muscle weights of the tibialis anterior (TA) (C), gastrocnemius (GA) (D), and quadriceps femoris (QD) (E) were measured and normalized to body weight (n = 8–10 in each group) (F) A representative picture of H&E staining. Scale bar = 50 μm (n = 3 in each group) (G) The cross-sectional area (CSA) of muscle fibers was measured by ImageJ software (H) Muscle fiber size distribution (I) A representative picture of Masson staining. Scale bar = 100 μm (n = 3 in each group) (J) Quantitative analysis of the area of fibrosis using ImageJ software (K–M) The protein expression levels of MuRF1 and atrogin-1 were detected by Western blot (n = 3 in each group). GAPDH was used as an internal control. The relative protein expression level was quantified by ImageJ software. Data are presented as the mean ± SD, $^{*}p < 0.05$, $^{**}p < 0.01$, $^{***}p < 0.001$.

abundant expression in all four datasets (Fig. 7G). Among them, miR-132-3p plays an active role in various diseases, which can promote diabetic wound healing [22], improve cardiac dysfunction [26], relieve LPS-induced acute lung injury [27], and play a key role in neuron plasticity [28]. Moreover, studies have confirmed the existence of targeted binding sites between miR-132-3p and FoxO3(Fig. 7H) [29]. Therefore, we investigated the role of miR-132-3p in muscle atrophy. Our study found that the expression level of miR-132-3p decreased after dexamethasone treatment and increased after hucMSC-Exos treatment (Fig. 7I and J). To further investigate the mechanism of hucMSC-Exos in treating myotube atrophy, we loaded the mimic negative control, miR-132-3p mimics, the inhibitor negative control, and miR-132-3p inhibitor into hucMSC-Exos, compared to the mimic negative control, miR-132-3p mimic-loaded hucMSC-Exos further reduced the dexamethasone-induced up-regulation of MuRF1, atrogin-1, and FoxO3. Conversely, the miR-132-3p inhibitor-loaded hucMSC-Exos attenuated the salvage effect of hucMSC-Exos on dexamethasone-induced myotube atrophy compared to the inhibitor-negative control (Fig. 7K–N). These results suggest that hucMSC-Exos may ameliorate muscle atrophy via the miR-132-3p/FoxO3 axis.

4. Discussion

Sarcopenia can impair physical function and increase the risk of falls, which can affect quality of life [30]. Excessive muscle mass reduction can contribute to increased morbidity and mortality. However, apart from exercise and diet, there is no effective treatment for sarcopenia. Therefore, it is crucial to explore effective treatments for sarcopenia. In this study, hucMSC-Exos were effective in improving age-related and dexamethasone-induced muscle atrophy. FoxO3 plays an important role in the regulation of muscle protein degradation, and hucMSC-Exos may reduce the expression of FoxO3 through the release of miR-132-3p, thereby improving muscle atrophy.

To investigate the role of hucMSC-Exos in sarcopenia, we used two animal models of muscle atrophy where exosomes were injected into mice via the tail vein, and the results suggested that exosomes may be an effective strategy for the treatment of muscle atrophy. Although prior studies have shown that exosomes can treat muscle atrophy. Bone marrow MSC-Exos attenuated the decrease of myotube diameter and inhibited dexamethasone-induced muscle atrophy [31]. HucMSC-Exos treatment can effectively improve diabetes-induced muscle atrophy [32]. However, hucMSC-Exos have not been reported for the treatment of age-related and dexamethasone-induced muscle atrophy. Furthermore, animal models of age-related and dexamethasone-induced muscle atrophy exhibit similar phenotypic changes, particularly in terms of body composition and physical performance [33]. Our results showed that hucMSC-Exos therapy improved muscle mass and function. HucMSC-Exos treatment did not affect the weight of mice, but the weight loss of various muscle tissues, such as GA, TA, and QD, was inhibited by hucMSC-Exos treatment. In line with this, hucMSC-Exos treatment improved grip strength, increased muscle fiber cross-sectional area, and reduced the development of muscle fibrosis in age-related and dexamethasone-induced muscle atrophy. There are two main types of skeletal muscle fibers: slow muscle fibers and fast muscle fibers. The study showed that age-related and dexamethasone-induced muscle atrophy mice reduced fast muscle fibers first, rather than slow muscle fibers, resulting in a shift in muscle type from fast to slow [34]. The GA is a hybrid muscle composed of both slow and fast muscle fibers [35], so we used the GA muscle for the experiment. In this study, we found that muscle atrophy-related factors (MuRF1 and atrogin-1) significantly increased in two muscle atrophy animal models while hucMSC-Exos treatment reduced their protein levels. These results strongly indicate that hucMSC-Exos therapy effectively improved age-related and dexamethasone-induced muscle atrophy.

Exosomes play an important role in intercellular and interorgan communication, contributing significantly to angiogenesis and the treatment of diabetes and related diseases. Studies have reported that exosomes can regulate the proliferation and migration of vascular smooth muscle cells in vitro [36]. In a diabetic model, exosome treatment promoted the regeneration of islet cells and improved islet function, thereby maintaining a stable blood glucose state [37]. Exosomes can improve diabetic wound closure and angiogenesis by improving the proliferation, migration, and angiogenesis potential of human keratinocytes [38]. In this study, hucMSC-Exos can promote C2C12 cell proliferation and improve the decline in the viability of C2C12 myotubes caused by dexamethasone. In addition, in a cell model of dexamethasone-induced myotubes atrophy, hucMSC-Exos can rescue the dexamethasone-induced myotubes diameter reduction and reduce the expression of atrogin-1 and MuRF1. These in vitro findings indicated that hucMSC-Exos can rescue dexamethasone-induced myotubes atrophy.

To elucidate the potential molecular mechanism of hucMSC-Exos in the treatment of muscle atrophy, transcriptome sequencing was performed on the dexamethasone-induced group and the control-treated group. The KEGG pathway analysis revealed two signaling pathways closely related to muscle atrophy: the FoxO signaling pathway and the PI3K-AKT signaling pathway. Down-regulation of the PI3K-AKT signaling pathway leads to decreased FoxO protein phosphorylation and dephosphorylated FoxO enters into the nucleus, thereby increasing the expression levels of MuRF1 and atrogin-1, and promoting muscle atrophy [24]. Therefore, we next explored the role of the FoxO family in the use of hucMSC-Exos to treat muscle atrophy. Studies have shown that Forkhead box class O family member proteins (FoxOs) are highly conserved transcription factors that play an important role in the regulation of skeletal muscle protein degradation. FoxOs can regulate muscle proteolytic systems, namely the ubiquitin-proteasome system and autophagy-lysosome system [39]. Atrogin-1 and MuRF1 are also involved in the FoxO signaling pathway, and these two ubiquitin ligases are overexpressed in various atrophy models such as fasting, denervation, aging, and diabetes [39]. Our study demonstrated that hucMSC-Exos therapy reduced the dexamethasone-induced increases in FoxO3 expression levels. HucMSC-Exos may rescue dexamethasone-induced muscle atrophy through FoxO3. Given the significant role of miRNAs in regulating muscle atrophy [40], we used the bioinformatics database TargetScan to search for FoxO3-targeting miRNAs and analyze the miRNAs enriched in hucMSC-Exos. Our results suggest that miR-132-3p, present in hucMSC-Exos, can ameliorate myotube atrophy by down-regulating FoxO3. Overexpression of miR-132-3p in hucMSC-Exos can further reduce the expression of factors related to myotube atrophy, while inhibition of miR-132-3p in hucMSC-Exos can reduce the salvage effect of hucMSC-Exos on myotube atrophy. Consequently, hucMSC-Exos may ameliorate muscle atrophy via the miR-132-3p/FoxO3 axis.

There are still several limitations in our study. First, skeletal muscle consists of two major types of muscle fibers: slow-twitch (type I) and fast-twitch (type II). Type II fibers can be further divided into type IIA,

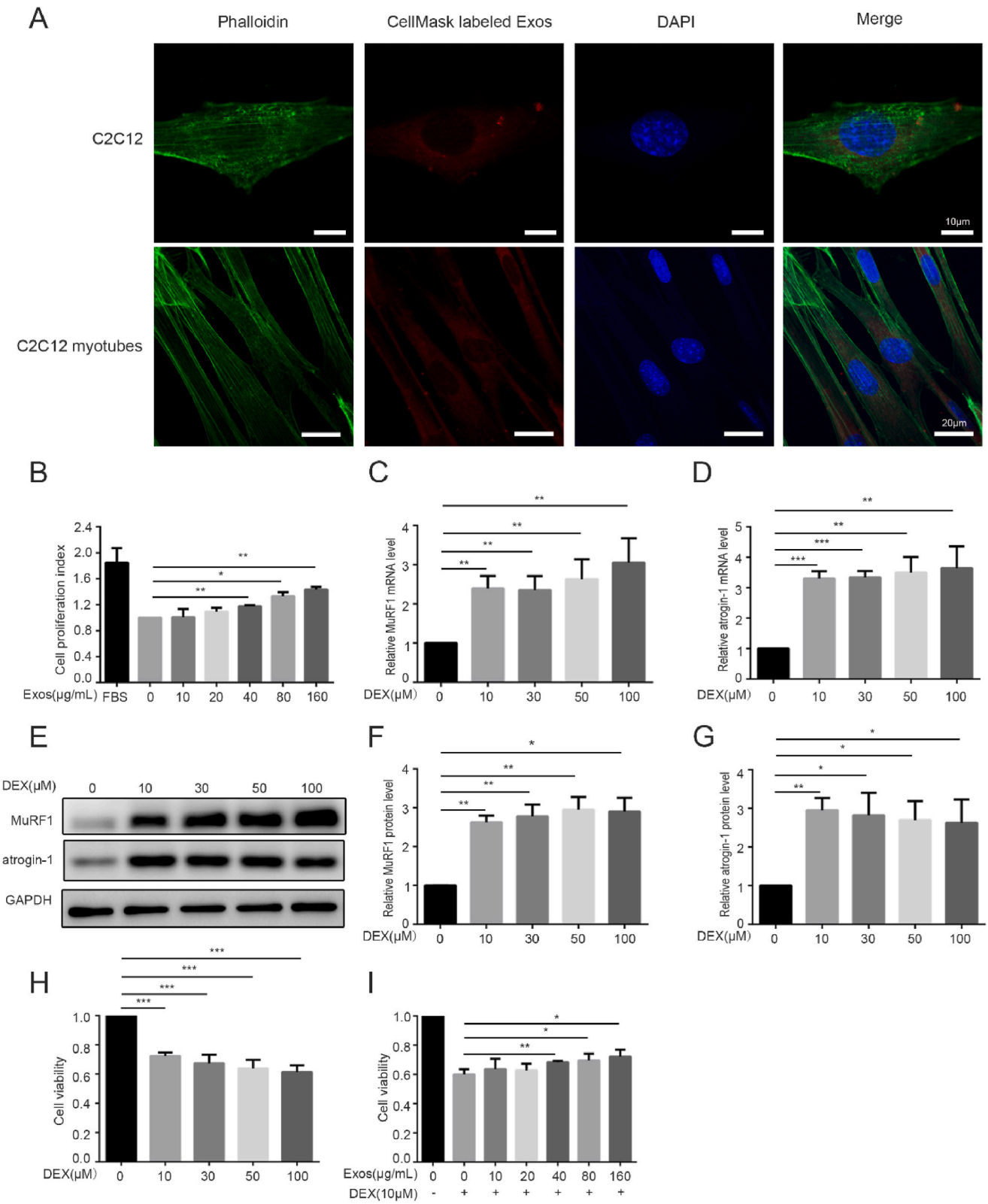

Figure 4. HucMSC-Exos promote the proliferation of C2C12 cells and rescue the dexamethasone-induced decline in the viability of C2C12 myotubes (A) HucMSC-Exos were labeled with CellMask (red) and co-cultured with C2C12 cells and C2C12 myotubes. For C2C12 cells, scale bar = 10 μm. For C2C12 myotubes, scale bar = 20 μm (B) Cell proliferation index of C2C12 cells treated with different concentrations of hucMSC-Exos (n = 3 in each group) (C) The mRNA expression level of MuRF1 treated with different concentrations of dexamethasone (n = 4 in each group) (D) The mRNA expression level of atrogin-1 treated with different concentrations of dexamethasone (n = 4 in each group) (E–G) The protein expression levels of MuRF1 and atrogin-1 were detected by Western blot (n = 3 in each group). GAPDH was used as an internal control. The relative protein expression level was quantified by ImageJ software (H) Cell viability of C2C12 myotubes treated with different concentrations of dexamethasone (n = 5 in each group) (I) Cell viability of C2C12 myotubes treated with dexamethasone and different concentrations of hucMSC-Exos (n = 4 in each group). Data are presented as the mean ± SD, $*p < 0.05$, $**p < 0.01$, $***p < 0.001$.

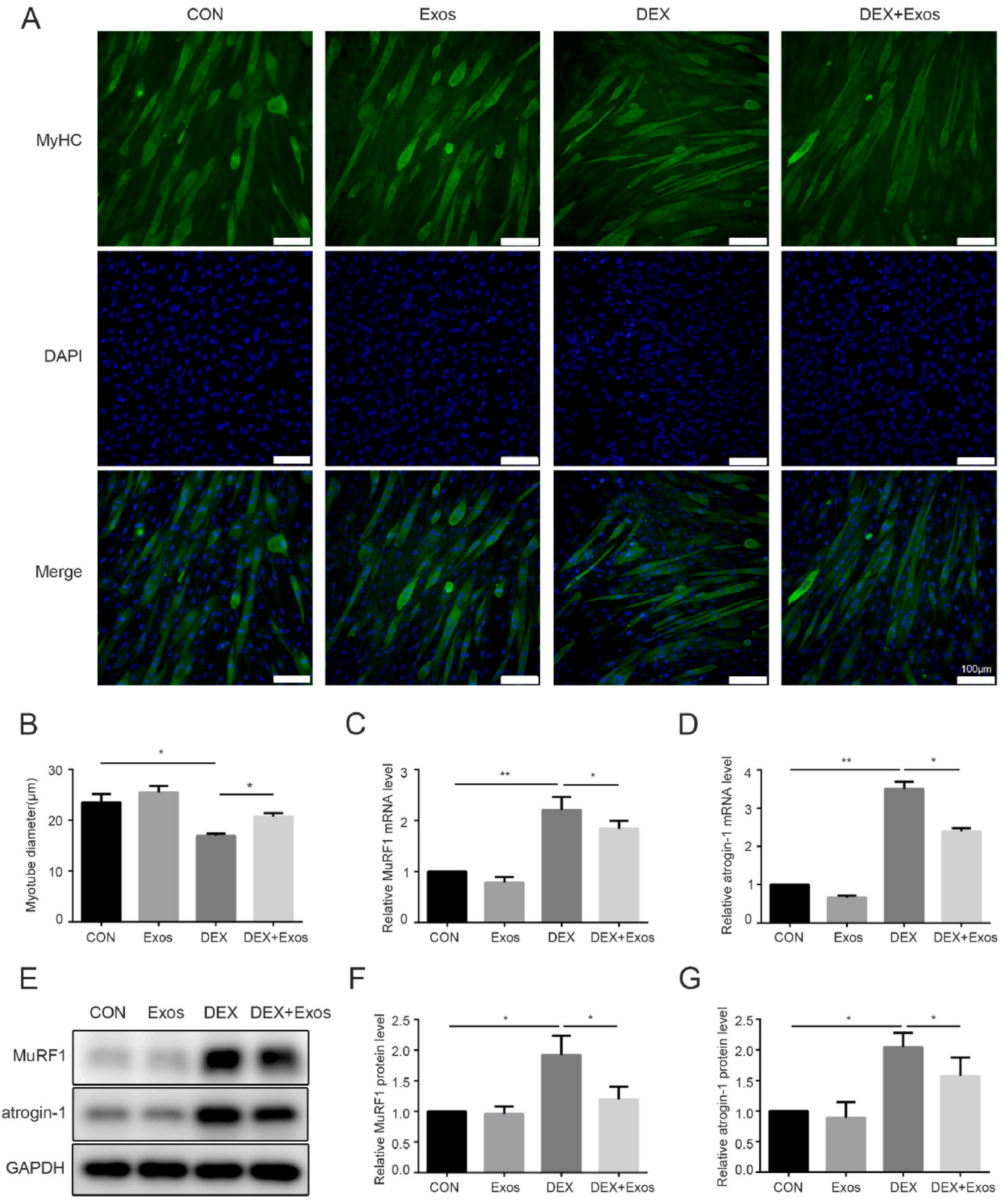

Figure 5. HucMSC-Exos rescue dexamethasone-induced myotube atrophy (A) Immunofluorescence staining of MyHC in C2C12 myotubes with the treatment of dexamethasone and hucMSC-Exos. Scale bar = 100 μm (n = 3 in each group) (B) The C2C12 myotube diameters were quantified using ImageJ software (C, D) The mRNA expression level of MuRF1 and atrogin-1 (n = 3 in each group) (E–G) The protein expression levels of MuRF1 and atrogin-1 were detected by Western blot (n = 3 in each group). GAPDH was used as an internal control. The relative protein expression level was quantified by ImageJ software. Data are presented as the mean ± SD, $^{*}p < 0.05$, $^{**}p < 0.01$.

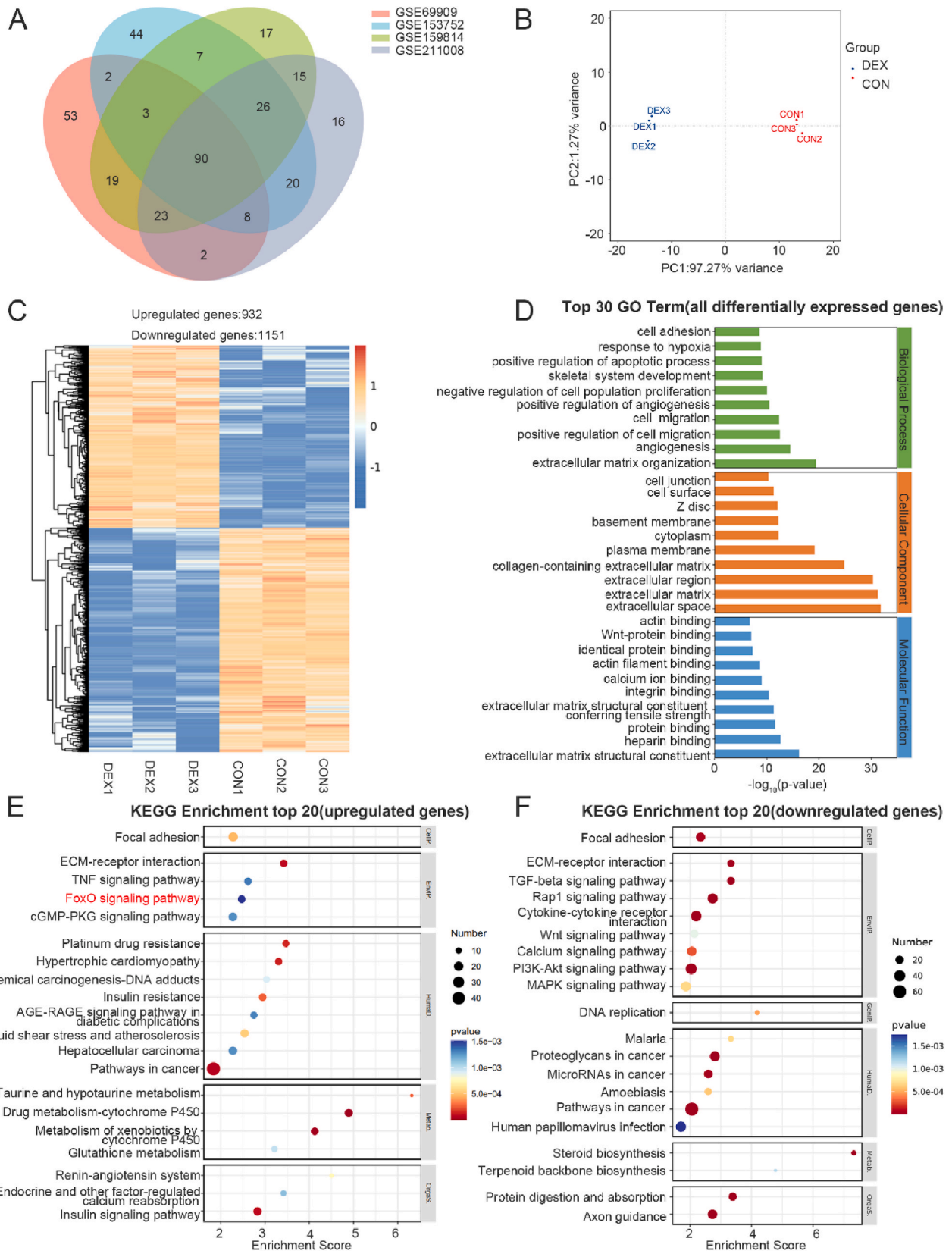

Figure 6. RNA sequence analysis for the dexamethasone and control groups (A) Venn diagram of the overlapped miRNAs of the top 200 miRNAs in GSE69909, GSE153752, GSE159814, and GSE211008 (B) Principal component analysis (PCA) was analyzed from RNA sequence data between the dexamethasone and control groups (C) Heatmap of differential expression genes between the dexamethasone and control groups (D) Top 30 GO terms of GO enrichment analysis based on differential expression genes (E) Top 20 functionally enriched KEGG pathway analysis based on upregulated genes (F) Top 20 functionally enriched KEGG pathway analysis based on downregulated genes. Cellp.: Cellular Processes, EnVIP.: Environmental Information Processing, GenIP.: Genetic Information Processing , HumaD.: Human Diseases , Metab.: Metabolism , OrgaS.: Organismal Systems.

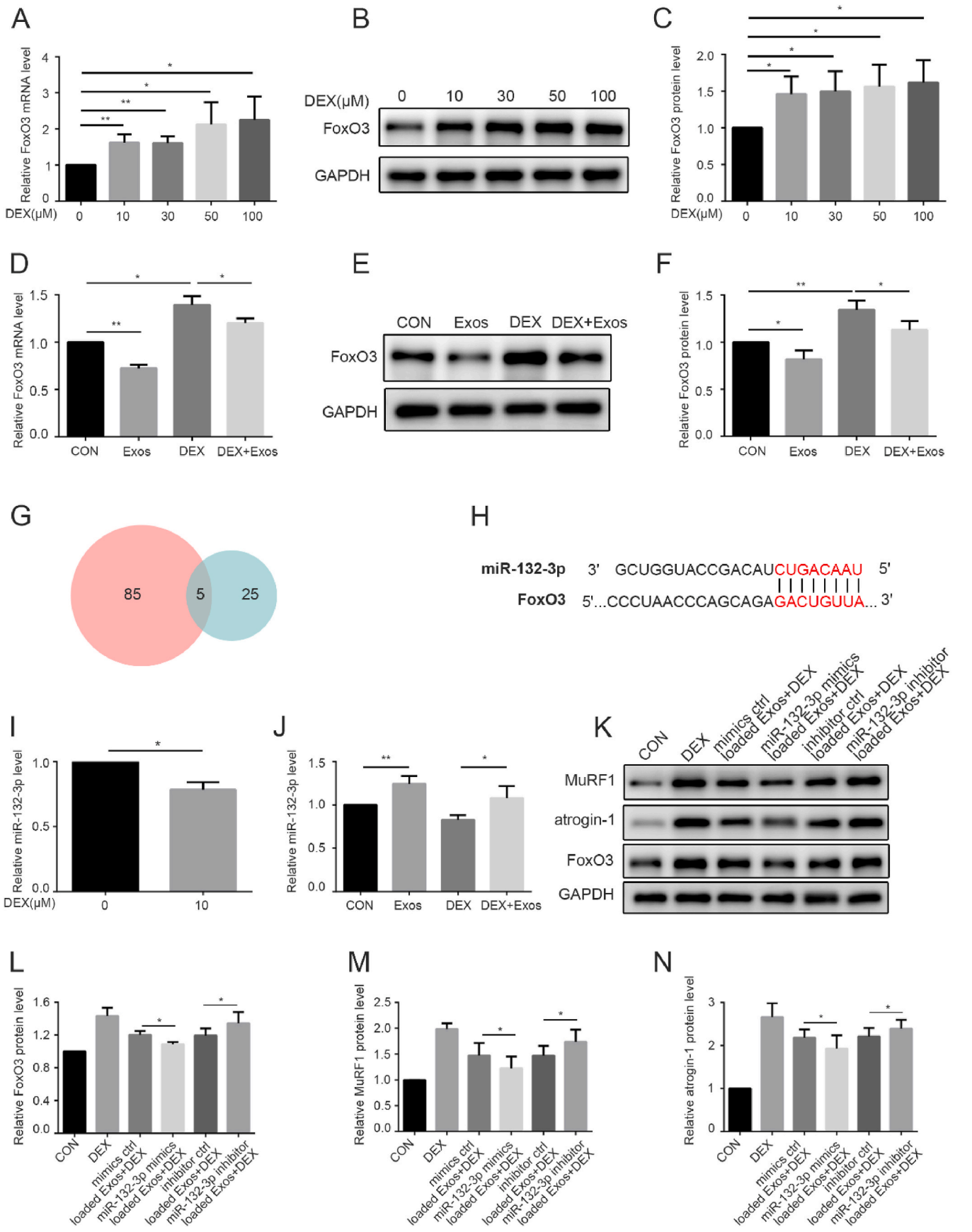

(caption on next page)

Figure 7. MiR-132-3p derived from hucMSC-Exos inhibits dexamethasone-induced myotube atrophy by targeting FoxO3 (A) The mRNA expression level of FoxO3 treated with different concentrations of dexamethasone (n = 5 in each group) (B, C) The protein expression level of FoxO3 was detected by Western blot (n = 4 in each group). GAPDH was used as an internal control. The relative protein expression level was quantified by ImageJ software (D) The mRNA expression level of FoxO3 (n = 3 in each group) (E, F) The protein expression level of FoxO3 was detected by Western blot (n = 4 in each group). GAPDH was used as an internal control. The relative protein expression level was quantified by ImageJ software (G) Venn diagram of the overlapped miRNAs with conserved binding sites to FoxO3 and abundant expression in all four datasets. The pink circles represented abundantly expressed miRNAs in all four datasets (GSE69909, GSE153752, GSE159814, and GSE211008). The light green represented the miRNAs with conserved binding sites to FoxO3 (H) The binding sites between miR-132-3p and FoxO3 mRNA have been reported (I, J) The expression level of miR-132-3p (n = 3 in each group) (K–N) The protein expression levels of MuRF1, atrogin-1, and FoxO3 were detected by Western blot (n = 3 in each group). GAPDH was used as an internal control. The relative protein expression level was quantified by ImageJ software. Data are presented as the mean ± SD, $*p < 0.05$, $**p < 0.01$.

type IIB, and IIX fibers [41]. We did not fully explore the effect of hucMSC-Exos on all types of fibers in GA. In future studies, we will further investigate the effect of hucMSC-Exos on muscle fiber types. Second, IRS-1 ubiquitination regulates muscle protein anabolism and catabolism [42]. We did not investigate whether hucMSC-Exos improved muscle atrophy by modulating IRS-1 ubiquitination. Third, hucMSCs can ameliorate age-related muscle atrophy by modulating inflammation and apoptosis [43]. We did not evaluate whether hucMSC-Exos improved muscle atrophy by regulating inflammation and apoptosis. Further research is needed to explore these issues.

5. Conclusion

In summary, we first validated the effectiveness of hucMSC-Exos therapy through two animal models of age-related and dexamethasone-induced muscle atrophy. Further, we found that hucMSC-Exos may ameliorate muscle atrophy via the miR-132-3p/FoxO3 axis. This indicates that the application of hucMSC-Exos can alleviate muscle atrophy and provide a novel and promising therapeutic method for the treatment of sarcopenia.

Funding

This work was supported by grants from the National Natural Science Foundation of China (No. 82170894), the Science and Technology Commission of Shanghai Municipality (21S11901100), and the Research Physician Project of Shanghai Tenth People's Hospital (2023YJXYSA014).

Data availability

Data will be made available on request.

Declaration of competing interest

Huihui Ma, Yujie Jing, Jiangping Zeng, Jiaying Ge, Siqi Sun, Ran Cui, Chunhua Qian, Shen Qu, and Hui Sheng declare that they have no conflict of interest.

Acknowledgments

The authors would like to thank the support of experimental equipment in the center laboratory of Shanghai Tenth People's Hospital.

References

[1] Jones G, Trajanoska K, Santanasto AJ, Stringa N, Kuo C-L, Atkins JL, et al. Genome-wide meta-analysis of muscle weakness identifies 15 susceptibility loci in older men and women. Nat Commun 2021;12(1):654 [eng].
[2] Webb EK, Ng SY, Mikhail AI, Stouth DW, vanLieshout TL, Syroid AL, et al. Impact of short-term, pharmacological CARM1 inhibition on skeletal muscle mass, function, and atrophy in mice. Am J Physiol Endocrinol Metab 2023;325(3):E252–66 [eng].
[3] Dave S, Patel BM. Deliberation on debilitating condition of cancer cachexia: skeletal muscle wasting. Fundam Clin Pharmacol 2023 [eng].
[4] Bielecka-Dabrowa A, Fabis J, Mikhailidis DP, von Haehling S, Sahebkar A, Rysz J, et al. Prosarcopenic effects of statins may limit their effectiveness in patients with heart failure. Trends Pharmacol Sci 2018;39(4):331–53 [eng].
[5] Yeung SSY, Reijnierse EM, Pham VK, Trappenburg MC, Lim WK, Meskers CGM, et al. Sarcopenia and its association with falls and fractures in older adults: a systematic review and meta-analysis. J Cachexia Sarcopenia Muscle 2019;10(3):485–500 [eng].
[6] Chen L-K, Woo J, Assantachai P, Auyeung T-W, Chou M-Y, Iijima K, et al. Asian working group for sarcopenia: 2019 consensus update on sarcopenia diagnosis and treatment. J Am Med Dir Assoc 2020;21(3) [eng].
[7] Kang Y-J, Yoo J-I, Baek K-W. Differential gene expression profile by RNA sequencing study of elderly osteoporotic hip fracture patients with sarcopenia. J Orthop Translat 2021;29:10–8 [eng].
[8] Sjöblom S, Suuronen J, Rikkonen T, Honkanen R, Kröger H, Sirola J. Relationship between postmenopausal osteoporosis and the components of clinical sarcopenia. Maturitas 2013;75(2):175–80 [eng].
[9] Zhang H-W, Tsai Z-R, Chen K-T, Hsu S-L, Kuo Y-J, Lin Y-C, et al. Enhanced risk of osteoporotic fracture in patients with sarcopenia: a national population-based study in taiwan. J Personalized Med 2022;12(5) [eng].
[10] Yaghoubi Y, Movassaghpour A, Zamani M, Talebi M, Mehdizadeh A, Yousefi M. Human umbilical cord mesenchymal stem cells derived-exosomes in diseases treatment. Life Sci 2019;233:116733 [eng].
[11] Feng H, Liu Q, Deng Z, Li H, Zhang H, Song J, et al. Human umbilical cord mesenchymal stem cells ameliorate erectile dysfunction in rats with diabetes mellitus through the attenuation of ferroptosis. Stem Cell Res Ther 2022;13(1):450 [eng].
[12] Li T, Yan Y, Wang B, Qian H, Zhang X, Shen L, et al. Exosomes derived from human umbilical cord mesenchymal stem cells alleviate liver fibrosis. Stem Cell Dev 2013;22(6):845–54 [eng].
[13] Zhu Y-G, Feng X-M, Abbott J, Fang X-H, Hao Q, Monsel A, et al. Human mesenchymal stem cell microvesicles for treatment of Escherichia coli endotoxin-induced acute lung injury in mice. Stem Cell 2014;32(1):116–25 [eng].
[14] Yang D, Zhang W, Zhang H, Zhang F, Chen L, Ma L, et al. Progress, opportunity, and perspective on exosome isolation - efforts for efficient exosome-based theranostics. Theranostics 2020;10(8):3684–707 [eng].
[15] Kalluri R, LeBleu VS. The biology, function, and biomedical applications of exosomes. Science 2020;367(6478) [eng].
[16] Zargar MJ, Kaviani S, Vasei M, Soufi Zomorrod M, Heidari Keshel S, Soleimani M. Therapeutic role of mesenchymal stem cell-derived exosomes in respiratory disease. Stem Cell Res Ther 2022;13(1):194 [eng].
[17] Qin D, Wang C, Li D, Guo S. Exosomal miR-23a-3p derived from human umbilical cord mesenchymal stem cells promotes remyelination in central nervous system demyelinating diseases by targeting Tbr1/Wnt pathway. J Biol Chem 2023:105487 [eng].
[18] Li Z, Liu Y, Tian Y, Li Q, Shi W, Zhang J, et al. Human umbilical cord mesenchymal stem cell-derived exosomes improve ovarian function in natural aging by inhibiting apoptosis. Int J Mol Med 2023;52(4) [eng].
[19] Gebert LFR, MacRae IJ. Regulation of microRNA function in animals. Nat Rev Mol Cell Biol 2019;20(1):21–37 [eng].
[20] Xu S, Cheuk YC, Jia Y, Chen T, Chen J, Luo Y, et al. Bone marrow mesenchymal stem cell-derived exosomal miR-21a-5p alleviates renal fibrosis by attenuating glycolysis by targeting PFKM. Cell Death Dis 2022;13(10):876 [eng].
[21] Lee M-K, Choi J-W, Choi YH, Nam T-J. Pyropia yezoensis protein prevents dexamethasone-induced myotube atrophy in C2C12 myotubes. Mar Drugs 2018;16(12) [eng].
[22] Ge L, Wang K, Lin H, Tao E, Xia W, Wang F, et al. Engineered exosomes derived from miR-132-overexpresssing adipose stem cells promoted diabetic wound healing and skin reconstruction. Front Bioeng Biotechnol 2023;11:1129538 [eng].
[23] Cao M, Zhao Y, Chen T, Zhao Z, Zhang B, Yuan C, et al. Adipose mesenchymal stem cell-derived exosomal microRNAs ameliorate polycystic ovary syndrome by protecting against metabolic disturbances. Biomaterials 2022;288:121739 [eng].
[24] Sandri M, Sandri C, Gilbert A, Skurk C, Calabria E, Picard A, et al. Foxo transcription factors induce the atrophy-related ubiquitin ligase atrogin-1 and cause skeletal muscle atrophy. Cell 2004;117(3):399–412 [eng].
[25] Bodine SC, Baehr LM. Skeletal muscle atrophy and the E3 ubiquitin ligases MuRF1 and MAFbx/atrogin-1. Am J Physiol Endocrinol Metab 2014;307(6):E469–84 [eng].
[26] Wang G, Wang R, Ruan Z, Liu L, Li Y, Zhu L. MicroRNA-132 attenuated cardiac fibrosis in myocardial infarction-induced heart failure rats. Biosci Rep 2020;40(9) [eng].
[27] Liu J-H, Cao L, Zhang C-H, Li C, Zhang Z-H, Wu Q. Dihydroquercetin attenuates lipopolysaccharide-induced acute lung injury through modulating FOXO3-mediated NF-κB signaling via miR-132-3p. Pulm Pharmacol Ther 2020;64:101934 [eng].

[28] Ma X, Wang Y, Shi Y, Li S, Liu J, Li X, et al. Exosomal miR-132-3p from mesenchymal stromal cells improves synaptic dysfunction and cognitive decline in vascular dementia. Stem Cell Res Ther 2022;13(1):315 [eng].
[29] Mehta A, Zhao JL, Sinha N, Marinov GK, Mann M, Kowalczyk MS, et al. The MicroRNA-132 and MicroRNA-212 cluster regulates hematopoietic stem cell maintenance and survival with age by buffering FOXO3 expression. Immunity 2015;42(6):1021–32 [eng].
[30] Ge J, Zeng J, Ma H, Sun S, Zhao Z, Jing Y, et al. A new index based on serum creatinine and cystatin C can predict the risks of sarcopenia, falls and fractures in old patients with low bone mineral density. Nutrients 2022;14(23) [eng].
[31] Li Z, Liu C, Li S, Li T, Li Y, Wang N, et al. BMSC-derived exosomes inhibit dexamethasone-induced muscle atrophy via the miR-486-5p/FoxO1 Axis. Front Endocrinol 2021;12:681267 [eng].
[32] Song J, Liu J, Cui C, Hu H, Zang N, Yang M, et al. Mesenchymal stromal cells ameliorate diabetes-induced muscle atrophy through exosomes by enhancing AMPK/ULK1-mediated autophagy. J Cachexia Sarcopenia Muscle 2023;14(2): 915–29 [eng].
[33] Wang BY-H, Hsiao AW-T, Wong N, Chen Y-F, Lee C-W, Lee WYW. Is dexamethasone-induced muscle atrophy an alternative model for naturally aged sarcopenia model? J Orthop Translat 2023;39:12–20 [eng].
[34] Seo E, Truong C-S, Jun H-S, Psoralea corylifolia L. Seed extract attenuates dexamethasone-induced muscle atrophy in mice by inhibition of oxidative stress and inflammation. J Ethnopharmacol 2022;296:115490 [eng].
[35] Shen S, Liao Q, Liu J, Pan R, Lee SM-Y, Lin L. Myricanol rescues dexamethasone-induced muscle dysfunction via a sirtuin 1-dependent mechanism. J Cachexia Sarcopenia Muscle 2019;10(2):429–44 [eng].
[36] Liu R, Shen H, Ma J, Sun L, Wei M. Extracellular vesicles derived from adipose mesenchymal stem cells regulate the phenotype of smooth muscle cells to limit intimal hyperplasia. Cardiovasc Drugs Ther 2016;30(2):111–8 [eng].
[37] Nojehdehi S, Soudi S, Hesampour A, Rasouli S, Soleimani M, Hashemi SM. Immunomodulatory effects of mesenchymal stem cell-derived exosomes on experimental type-1 autoimmune diabetes. J Cell Biochem 2018;119(11):9433–43 [eng].
[38] Wang J-W, Zhu Y-Z, Ouyang J-Y, Nie J-Y, Wang Z-H, Wu S, et al. Adipose-derived stem cell extracellular vesicles improve wound closure and angiogenesis in diabetic mice. Plast Reconstr Surg 2023;151(2):331–42 [eng].
[39] Sanchez AMJ, Candau RB, Bernardi H. FoxO transcription factors: their roles in the maintenance of skeletal muscle homeostasis. Cell Mol Life Sci 2014;71(9):1657–71 [eng].
[40] Yu Y, Chu W, Chai J, Li X, Liu L, Ma L. Critical role of miRNAs in mediating skeletal muscle atrophy (Review) Mol Med Rep 2016;13(2):1470–4 [eng].
[41] Wang BY-H, Hsiao AW-T, Shiu HT, Wong N, Wang AY-F, Lee C-W, et al. Mesenchymal stem cells alleviate dexamethasone-induced muscle atrophy in mice and the involvement of ERK1/2 signalling pathway. Stem Cell Res Ther 2023;14 (1):195 [eng].
[42] Meng X, Huang Z, Inoue A, Wang H, Wan Y, Yue X, et al. Cathepsin K activity controls cachexia-induced muscle atrophy via the modulation of IRS1 ubiquitination. J Cachexia Sarcopenia Muscle 2022;13(2):1197–209 [eng].
[43] Piao L, Huang Z, Inoue A, Kuzuya M, Cheng XW. Human umbilical cord-derived mesenchymal stromal cells ameliorate aging-associated skeletal muscle atrophy and dysfunction by modulating apoptosis and mitochondrial damage in SAMP10 mice. Stem Cell Res Ther 2022;13(1):226 [eng].